Polyhedron 28 (2009) 1049–1056

Contents lists available at ScienceDirect

Polyhedron

journal homepage: www.elsevier.com/locate/poly

Kinetics and mechanism of the chromic oxidation of 3-*O*-methyl-D-glucopyranose

María Inés Frascaroli [a], Juan Manuel Salas-Peregrin [b], Luis F. Sala [a,*], Sandra Signorella [a,*]

[a] Instituto de Química Rosario – CONICET, Universidad Nacional de Rosario, Suipacha 531, S2002LRK Rosario, Argentina
[b] Departamento de Química Inorgánica, Facultad de Ciencias, Universidad de Granada, Fuentenueva s/n, 18071 Granada, Spain

ARTICLE INFO

Article history:
Received 26 September 2008
Accepted 7 January 2009
Available online 21 March 2009

Keywords:
Chromate
3-*O*-methylglucose
Redox chemistry
Kinetics

ABSTRACT

The oxidation of 3-*O*-methyl-D-glucopyranose (Glc3Me) by Cr^{VI} in acid medium yields Cr^{III}, formic acid and 2-*O*-methyl-D-arabinose as final products when a 50-times or higher excess of Glc3Me over Cr^{VI} is used. The redox reaction takes place through the combination of $Cr^{VI} \rightarrow Cr^{IV} \rightarrow Cr^{II}$ and $Cr^{VI} \rightarrow Cr^{IV} \rightarrow Cr^{III}$ pathways. Intermediacy of free radicals and Cr^{II} in the reaction was demonstrated by the observation of induced polymerization of acrylamide and detection of CrO_2^{2+} formed by reaction of Cr^{II} with O_2. Intermediate oxo-Cr^{V}–Glc3Me species were detected by EPR spectroscopy. In 0.3–0.5 mol/L $HClO_4$, intermediate Cr^{V} rapidly decompose to the reaction products, while, at pH 5.5–7.5, where the redox processes are very slow, five-coordinate Cr^{V} bis-chelates of the pyranose and furanose forms of Glc3Me remain more than 15 h in solution. The C1–C2 bond cleavage of Glc3Me upon reaction with Cr^{VI} distinguishes this derivative from glucose, which is oxidized to gluconic acid.

1. Introduction

Compounds of Cr^{VI} are dangerous pollutants used and generated by industries [1]. Due to the carcinogenic and toxic effects of Cr^{VI} [2,3], and the fact that intermediate oxidation states generated during the reduction of Cr^{VI} to Cr^{III} may be implied in the mechanism of Cr–induced cancers [4], studies on the kinetics and mechanism of the oxidation of biologically relevant reducing agents by Cr^{VI} is of interest to both biochemists and inorganic chemists [4–6]. Compounds such as polyalcohols and hydroxycarboxylic acids, are effective as nonenzymatic reductants (at low pH) and can stabilize the labile oxidation states of chromium [4,7–9]. Therefore, polyoxygenated compounds may play an important role in chromate toxicity. Because of their potential biological and ecological relevance there is an increasing interest in studying the stabilization/reduction of hypervalent chromium by saccharides. Previous studies on the oxidation of aldoses [10,11], 2-deoxy-aldoses [11–13] and 6-deoxy-aldoses [10,14] by Cr^{VI} showed that the C1–OH hemiacetalic function reacts faster than the primary or any of the secondary alcoholic groups, to yield the corresponding aldonic acid as the only reaction product. These works provided information on the role of C2–OH and, in lesser extent, C6–OH, to act as chelating sites of Cr^{VI} to form chromate ester intermediates that retard the oxidation of C1–OH, and established that an equatorial 3-OH group has none or negligible influence on the reaction kinetics and mechanism. In the present work, we study the reaction of Cr^{VI} with 3-*O*-methyl-D-glucopyranose (Glc3Me), and show that replacement of C3–OH by C3–OMe favors the C1–C2 bond cleavage over the formation of the aldonic acid, thus evidencing the "noninnocent" role of the OMe group at C3 of the sugar in the reaction with Cr^{VI}.

2. Experimental

2.1. Materials

3-*O*-methyl-D-glucopyranose (Sigma, 98%), potassium dichromate (Mallinckrodt), sodium chromate (Merck), perchloric acid (A.C.S. Baker), phosphoric acid (Anedra P.A.), sulfuric acid (Merck P.A.), glutathione (Sigma, 98–100%, reduced form), acrylamide (Sigma, >99%), *N*,*N*-dimethylformamide (Fisher Scientific), sodium hydroxide (Cicarelli, P.A.) were used without further purification.

Aqueous solutions were prepared in milliQ-deionized water (HPLC quality). For experiments performed at constant ionic strength (*I*) and different $[H^+]$, mixtures of $NaClO_4$ and $HClO_4$ solutions were prepared. The concentration of stock solutions of $HClO_4$ was determined by titration using standard analytical methods. 4-(2-Hydroxyethyl)-1-piperazineethanesulfonic acid (HEPES) buffer was used for experiments at pH 7.5. Acetate buffer was used for experiments at pH 5.5. $Na[Cr^{V}O(ehba)_2] \cdot H_2O$ and $Na_2[Cr^{IV}O(ehba)_2]$ were synthesized from 2-ethyl-2-hydroxybutanoic acid (ehba, Aldrich, 99%) according to literature methods [15,16].

Caution: Cr^{VI} compounds are human carcinogens, and Cr^{V} complexes are mutagenic and potential carcinogens [17]. Contact with skin and inhalation must be avoided. Acrylamide is a carcinogen and must be handled in a well-ventilated fume hood [18].

* Corresponding authors. Tel./fax: +54 341 4350214.
E-mail addresses: sala@iquir-conicet.gov.ar (L.F. Sala), signorel@infovia.com.ar (S. Signorella).

0277-5387/$ - see front matter © 2009 Elsevier Ltd. All rights reserved.
doi:10.1016/j.poly.2009.01.003

2.2. Methods

2.2.1. Product analysis

HPLC was employed to detect the reaction products under the conditions used in the kinetic measurements (excess of Glc3Me over Cr^{VI}). The chromatograms were obtained on a KNK-500 A chromatograph provided with a 7125 HPLC pump. The separation was carried out on a Supelcogel C-610H HPLC column (300×7.8 mm, Bio-Rad Laboratories) using 0.1% P/V H_3PO_4 as eluent and a flow rate of 0.5 mL/min, at 30 °C. The effluent was monitored with refractive index (ERC-7522, ERMA INC) and UV (115 UV Gilson, $\lambda = 220$ nm) detectors. The $[H^+]$ of the reaction mixtures (Glc3Me:Cr^{VI} ratios of 25:1, 50:1 and 100:1) was adjusted to 0.2 mol/L by addition of 2 mol/L $HClO_4$ and then the samples were filtered through a 0.2 μm membrane prior to injection into the chromatographic system.

Standard samples of 2-methyl-D-arabinose (Ara2Me), 3-methyl-D-gluconic acid (Glc3MeA) – prepared following published procedures [19,20] – and formic acid were prepared individually and the chromatographic retention times determined separately.

Chromatograms of the reaction mixtures showed two peaks with retention times (t_R) of 13′ 44″ and 17′ 11″, in addition to the peak of unreacted Glc3Me at t_R = 11′ 55″. The retention times of the new peaks are coincident with those of the standard solutions of Ara2Me and formic acid, respectively. No peak corresponding to Glc3MeA was detected in the reaction mixture. Furthermore, co-chromatography of a Cr^{VI}/Glc3Me reaction mixture and Ara2Me or formic acid resulted in the increase of peaks at 13′ 44″ or 17′ 11″, respectively. Additionally, the presence of HCO_2H acid was confirmed through the $HgCl_2$ reaction [21].

For the Glc3Me to Cr^{VI} ratios used in the kinetic studies (higher than 50:1), carbon dioxide was never detected as a reaction product.

2.2.2. Glc3Me stability

The stability of Glc3Me under conditions used in the kinetic studies was checked by monitoring the optical rotation changes on a JENA polarimeter with thermostated 20-cm tubes using the sodium D line. Reactant solutions were previously thermostated and transferred into the cell immediately after mixing. The optical rotations were recorded at different times after the preparation of the solutions and were identical to that of freshly prepared Glc3Me solutions. The specific rotation of Glc3Me was found to be $[\alpha]^{33}_D = +54.1° \pm 0.5°$ ($c = 3.88$ g/100 mL, 1.0 M $HClO_4$, $t = 10$ min to 30 h), a value similar to that measured for Glc3Me in aqueous solution: $[\alpha]^{20}_D = +55.7° \pm 0.5°$ ($c = 4.51$ g/100 mL).

The stability of the Glc3Me at 33 °C was also confirmed by HPLC after incubation of the solutions at fixed $[H^+]$.

2.2.3. Polymerization test

Polymerization of acrylamide was investigated during the reaction of Glc3Me with Cr^{VI} as a test for free radical generation. Acrylamide (0.6 g) was added to a reaction mixture containing $K_2Cr_2O_7$ (3×10^{-3} mmol) and Glc3Me (0.3 mmol) in 2 mL of 0.5 mol/L $HClO_4$, at 33 °C. When the color of Cr^{VI} disappeared, 1 mL of the mixture was diluted with 1 mL of methanol and a white polymer precipitated. Control experiments showed that no polymerization of acrylamide takes place under the experimental conditions with either $HCrO_4^-$ or the Glc3Me alone. The possible reaction of Cr^V or Cr^{IV} with acrylamide was tested with $Na[Cr^VO(ehba)_2]$ and $Na_2[Cr^{IV}O(ehba)_2]$. No precipitation occurred on mixing the Cr^V or Cr^{IV} complexes with acrylamide under the same conditions as those used in the Cr^{VI} + Glc3Me reaction.

2.2.4. Spectrophotometric measurements

Kinetic measurements were performed by monitoring absorbance changes using a Jasco V-550 UV/VIS spectrophotometer with a fully thermostated cell compartment (±0.2 °C). The reactions were followed under pseudo-first-order conditions, at 33 °C, using at least a 50-fold molar excess of Glc3Me over Cr^{VI} and different $[HClO_4]$. Reactant solutions were previously thermostated at 33 °C and transferred into a 1-cm pathlength cell immediately after mixing.

The disappearance of Cr^{VI} was followed spectrophotometrically at 350 nm until at least 80% conversion. In the kinetic measurements, the initial concentration of Cr^{VI} and I were kept constant at 8.0×10^{-4} mol/L and 1.02 mol/L, respectively, while $[HClO_4]$ was varied from 0.15 to 1.02 mol/L, at various [Glc3Me].

The experimental pseudo-first-order rate constants (k_{exp}), determined from the absorbance versus time curves at 350 nm, were deduced from multiple determinations and were within ±5% of each other. The first-order dependence of the rate upon $[Cr^{VI}]$ was verified in a set of experiments where the $[Cr^{VI}]_0$ was varied between 4.0×10^{-4} and 8.0×10^{-4} mol/L but T, $[Glc3Me]_0$, $[H^+]$ and I were kept constant.

The formation of Cr^{III} was monitored by following changes in the 570 nm absorption band. In these experiments the $[Cr^{VI}]_0$ was kept constant at 8.0×10^{-3} mol/L, (Glc3Me:Cr^{VI} ratio of 50) and the $[H^+]$ was varied between 0.40 and 1.02 mol/L. Rate constants obtained at this wavelength are in agreement with those calculated from data at 350 nm for the same experimental conditions.

Cr(VI) esters were investigated by UV–Vis spectrophotometry in the 350–500 nm region in which chromate esters show characteristic absorption bands. Reactions were performed at pH 3.52, where the redox reaction is slow enough to enable the observation of the ester formation. The instrument was zeroed to an arrangement of the reference and sample beams passing through matched cuvettes, both containing 6×10^{-4} mol/L Cr^{VI} at pH 3.52. The solution in the sample cell was replaced with the reaction solution containing 6×10^{-4} mol/L Cr^{VI} and 0.30–0.60 mol/L Glc3Me at pH 3.52, I = 1.02 M, and T = 33 °C. Spectra obtained within 40 min after mixing revealed a distinctive absorption at 373 nm.

The possible formation of Cr^{II} was examined by UV–Vis spectrophotometry in the 200–500 nm region in which CrO_2^{2+} show characteristic absorption bands. This experiment was performed at 22 °C, by periodic scanning of solutions containing 0.21 mol/L Glc3Me, 0.049 mmol/L Cr^{VI} and 1.26 mmol/L O_2, in 0.84 mol/L $HClO_4$. Under these conditions, the Cr^{VI} absorption band at 350 nm decreased in intensity, while new peaks at 293 nm and 247 nm, characteristic of CrO_2^{2+} [22], grew in.

2.2.5. EPR measurements

The EPR spectra were obtained on a Bruker EMX spectrometer operating at X-band frequencies (9–10 GHz). The microwave frequency was generated with a Bruker 04 ER and measured with a Bruker EMX 048T frequency meter. The magnetic field was measured with a Bruker EMX 035M NMR-probe gaussmeter. Spectra were recorded as first derivatives of the microwave absorption in 1024 points at ambient temperature (20 ± 1 °C). g-Values were determined by reference to diphenylpicryhydrazyl radical ($g = 2.0036$) as an external standard. Reactions were carried out by mixing Glc3Me and $K_2Cr_2O_7$ (ratio 49:1, $[Cr^{VI}] = 0.025$ mol/L) in 0.3 and 0.5 mol/L $HClO_4$; and by addition of $Na[Cr^VO(ehba)_2]$ (1.0 mmol/L), or Na_2CrO_4 (1.0 mmol/L) + glutathione (1.0 mmol/L), to solutions of Glc3Me (100 mmol/L) in acetate buffer (0.1 mol/L, pH 5.5) or HEPES buffer (0.1 mol/L, pH 7.5). Stock solution of $Na[Cr^VO(ehba)_2]$ (0.1 mol/L) was prepared in *N*,*N*-dimethylformamide. All of the EPR spectra were simulated using the program PEST WINSIM [23], assuming 100% Lorentzian line shapes.

The spectral parameters for each Cr^{V} species were consistent within all simulation, with maximum deviations in the g_{iso} values being ±0.0001 units. In the simulations, values for ^{1}H superhyperfine coupling constant a_H were included only where the a_H value was greater than the LW (line width) of the Cr^{V} species, since the signal is not significantly affected where the a_H value is ⩽LW.

3. Results and discussion

3.1. Products of the reaction of Glc3Me with Cr^{VI}

Under conditions used in the kinetic studies, excess of Glc3Me over Cr^{VI} in acid medium, HCO_2H and Ar2Me were identified by HPLC as the oxidation products of Glc3Me, while EPR and UV–Vis spectroscopies showed that aqueous Cr^{III} was the final Cr species in the reaction mixture. Thus, the reaction of Glc3Me and Cr^{VI} can be written as in Scheme 1.

This result implies that, in this reaction, C1–C2 bond break prevails over C1–H cleavage. A fact that differentiates the reactivity of the 3-*O*-methyl derivative towards Cr^{VI} from glucose that yields the corresponding aldonic acid as the only reaction product [10].

3.2. Detection of an intermediate Cr^{VI}-ester

At pH 3.52, the redox reaction of Cr^{VI} with Glc3Me proceeds very slowly, with negligible reduction of Cr^{VI} in the first 40 min. Thus, at this pH, the ester formation can be distinguished clearly from the electron transfer reaction. Differential UV–Vis spectra of mixtures of Cr^{VI} and Glc3Me exhibit, immediately after mixing, a distinctive absorption band with λ_{max} = 373 nm consistent with that ascribed to Cr^{VI} oxo-esters [24] that can be assigned to Glc3Me–Cr^{VI} species. Continued scanning over 40 min showed no further change in the spectra. The absorbance of this band increased with the increasing concentration of Glc3Me when the [Glc3Me] was varied at pH 3.5 (Fig. 1), probably as a result of a shift toward the ester in the esterification equilibrium.

3.3. Intermediacy of Cr^{II}

Involvement of Cr^{II} in the mechanism of the oxidation of a number of alcohols, saccharides and hydroxyacids by Cr^{IV} and Cr^{VI} in $HClO_4$ has been demonstrated by conversion into CrO_2^{2+} upon reaction with molecular oxygen [22,25–27]. At high [O_2] and low [Cr^{VI}] the reaction of Cr^{II} with O_2 can compete successfully with the reaction of Cr^{II} with Cr^{VI} and the autocatalytic consumption of CrO_2^{2+} by Cr^{II}, and if formed, Cr^{II} should yield the CrO_2^{2+} product [25,26,28,29]. We examined the presence of intermediate Cr^{II} in the reaction of Glc3Me with Cr^{VI}, by monitoring the formation of CrO_2^{2+}, using $[Cr^{VI}]_0$ low enough to avoid the Cr^{VI} + Cr^{II} competitive reaction. A periodic scanning of the O_2-saturated solution (1.26×10^{-3} mol/L O_2) of a Cr^{VI} + Glc3Me reaction mixture in 0.84 mol/L $HClO_4$ over a period of 3 h, showed that the band at 350 nm, characteristic of Cr^{VI}, decreased in intensity while two absorption bands at λ_{max} = 247 and 293 nm appeared (Fig. 2). These two bands are characteristic of CrO_2^{2+} formed as a long-lived intermediate [22] that then slowly transforms into the final Cr^{III}. Since

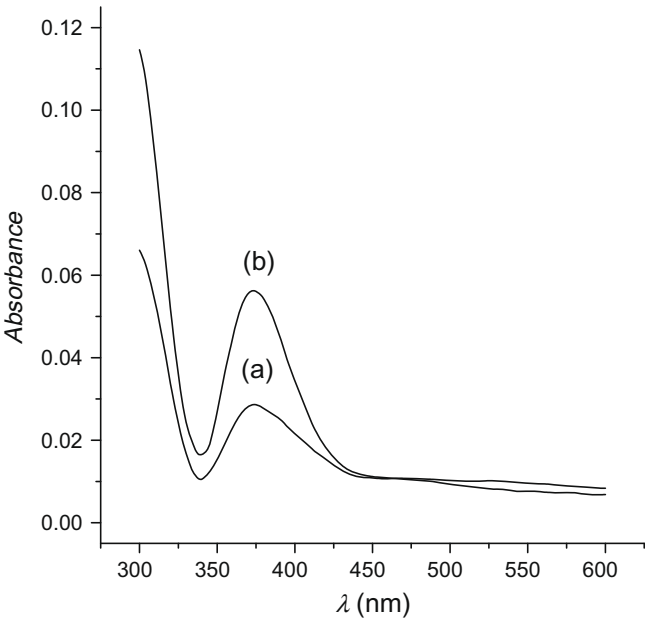

Fig. 1. UV–Vis difference spectra of Glc3Me/Cr^{VI} solutions at pH 3.52, showing the increasing band at 373 nm with increasing [Glc3Me]: (a) 0.30 and (b) 0.60 mol/L. $[Cr^{VI}] = 6.0 \times 10^{-4}$ mol/L, I = 1.02 mol/L, T = 33 °C. Spectra taken 30 min after preparation of the reaction mixture.

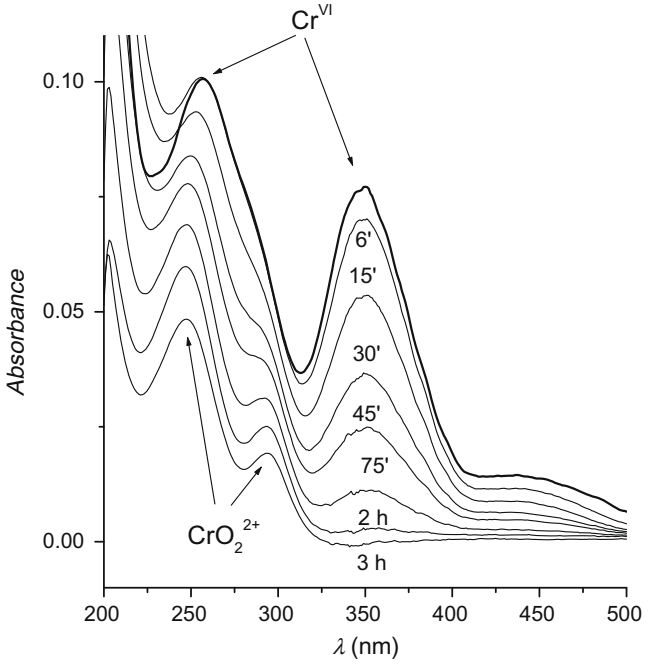

Fig. 2. Formation of CrO_2^{2+} (λ_{max} 293, 247) from the reaction between 0.21 mol/L Glc3Me, 1.26 mmol/L O_2 and 4.9×10^{-2} mmol/L Cr^{VI}, in 0.84 mol/L $HClO_4$. T = 22 °C.

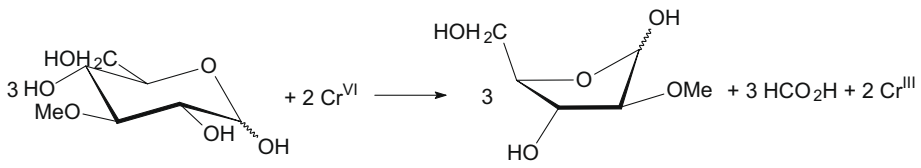

Scheme 1.

CrO_2^{2+} can be exclusively formed by reaction of Cr^{II} with O_2, and, in turn, Cr^{II} had previously been demonstrated to form exclusively through two-electron reduction of Cr^{IV} [26,28], our spectroscopic results provide evidence that Cr^{II} and Cr^{IV} are involved in the redox mechanism of the reaction between Cr^{VI} and Glc3Me.

3.4. Detection of intermediate Cr^V

The most common means of detecting Cr^V complexes in solution is EPR spectroscopy, where strong isotropic signals are observed at room temperature in X-band spectra. The reduction of Cr^V by Glc3Me is $[H^+]$ dependent, and at the high $[H^+]$ used in the kinetic measurements, Cr^V–Glc3Me redox processes are fast and, consequently, high modulation amplitude is required to observe Cr^V. With a modulation amplitude of 4 G, the EPR spectra of solutions from the reaction between Cr^{VI} and 50-times excess of Glc3Me in 0.3–0.5 mol/L $HClO_4$, consisted of two signals: a major one centered at g_{iso1} 1.9788, and an additional weak signal at g_{iso2} 1.9712 (Fig. 3) with relative intensity ⩽10% of the main signal. The high modulation amplitude used to observe Cr^V species at this $[H^+]$, disabled the resolution of the signal superhyperfine (shf) pattern (the ^1H shf splitting (a_H) for Cr^V–alcoholato species is usually <1 G [4,9]). Given that the g values of Cr^V species are very sensitive to the co-ordination number and the nature of the donor groups bound to Cr^V [4,9,30], an estimation of the intermediate Cr^V species formed in the reaction of Cr^{VI} with Glc3Me was made based on g_{iso} values of the EPR signals. The g_{iso} value of 1.9788 is typical of five-coordinate oxochromate(V) complexes formed with *O*-donor ligands, while the value of 1.9712 is typical of a six-co-ordinate oxo-Cr^V complex with two alcoholato donor sites and three water molecules, and can be assigned to $[Cr(O)(O^1,O^2\text{-Glc3Me})(H_2O)_3]^+$ (**I**, Fig. 4) [4,9,30]. The positive charge of this species is also consistent with its appearance at high $[H^+]$ and it is possibly responsible for the higher rates observed for the Cr^V–Glc3Me redox reactions at pH < 1.

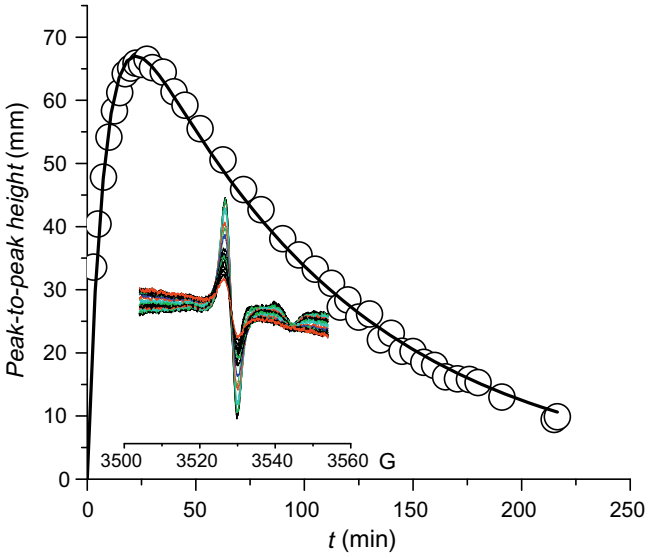

Fig. 3. Peak-to-peak heights of Cr^V EPR signals *vs.* time. $[Cr^{VI}] = 0.025$ mol/L, [Glc3Me] = 1.225 mol/L, $[H^+] = 0.3$ mol/L, $I = 1.02$ mol/L, $T = 20$ °C. Inset: time evolution of X-band EPR spectra from the reaction mixture in 0.3 mol/L $HClO_4$. $\nu = 9.766887$, mod. ampl. = 4 G.

At pH > 3 the redox reaction between Cr^V with Glc3Me becomes slow, Cr^V species remain in solution for longer periods of time and the shf pattern of the Cr^V EPR signals can be resolved using a modulation amplitude lower than the ^1H shf splitting. With this in mind, Cr^V–Glc3Me complexes formed upon addition of 100-times molar excess of Glc3Me to Cr^V generated in either the one-electron reduction of Cr^{VI} by glutathione or the ligand-exchange reaction of $[Cr^VO(ehba)_2]$ were investigated in the 5.5–7.5 pH range by EPR spectroscopy. The Cr^V EPR signals are more intense at pH 5.5 than at pH 7.5, probably because Cr^V disproportionation is slower at the lower pH [31]. In this pH range, the EPR spectra taken at the beginning of the reaction were dominated by a triplet at g_{iso1} 1.9792 ($a_H = 1.0 \times 10^{-4}$ cm^{-1}), with a minor component at g_{iso2} 1.9794 (quintet, $a_H = 0.9 \times 10^{-4}$ cm^{-1}). Fifteen minutes after mixing, the two components at g_{iso1} and g_{iso2} were present in 71% and 29%,

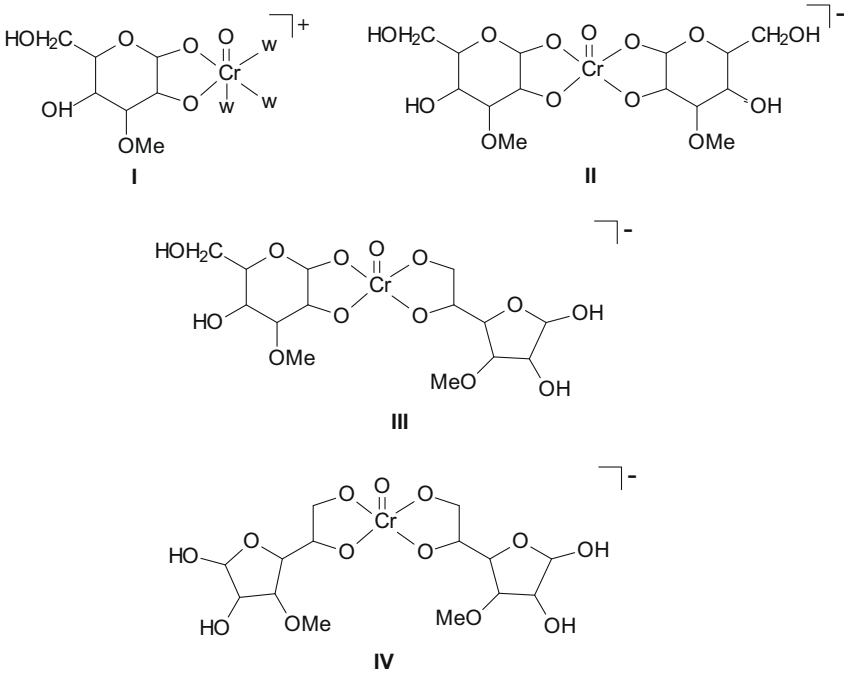

Fig. 4. Structures of Cr^V complexes formed with Glc3Me.

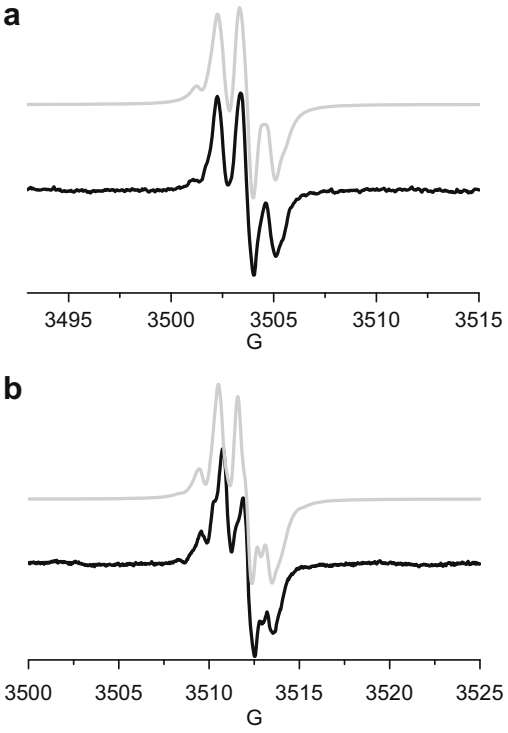

Fig. 5. Experimental (——) and simulated (——) X-band EPR spectra from mixtures of 1 mmol/L glutathione + 1mmol/L Cr^{VI} and 100 mmol/L Glc3Me, pH 5.5; taken (a) 15 min (ν = 9.705912 GHz) and (b) 1 h (ν = 9.728655) after mixing. Mod. ampl. = 0.2 G. T = 20 °C.

respectively (Fig. 5a). It is known that the EPR spectrum of a Cr^{V}-diolato species of six-membered ring *cis*-diols yields a doublet, since only one proton is in the plane of the unpaired electron density of the Cr^{V} ion. Consequently, the EPR spectral multiplicity of bis-chelate Cr^{V}-diolato$_2$ species formed between Cr^{V} and pyranosic *cis*-diols exhibit a triplet with two (one from each chelate ring) carbinolic protons coupled to the Cr^{V} electronic spin. In the present case, the major component of the EPR signal can be attributed to the bis-chelate [Cr(O)(*cis*-O^1,O^2-Glc3Me)$_2$] (**II**, Fig. 4). This result is in line with the reported higher ability of the *cis*- versus the *trans*-diolato for binding Cr^{V} [4,9,32]. The minor component at g_{iso2} 1.9794 can be attributed to the bis-chelate formed with the pyranose and furanose forms of Glc3Me: [Cr(O)(*cis*-O^1,O^2-Glc3Me)(O^5,O^6-Glc3Me-furanose)] (**III**, Fig. 4), with four protons coupled to the electronic spin of Cr^{V}. The assignment of the minor component to [Cr(O)(*cis*-O^1,O^2-Glc3Me-furanose)$_2$] was disregarded based on the a_H values – a_H values expected for Cr^{V}-diolato$_2$ species of five-membered ring *cis*-diols are lower than found here [33,34]. With time, the EPR spectral pattern slowly changed, the proportion of the components varied and a third component appeared. The EPR spectrum taken 1 h after mixing, shown in Fig. 5b, could be deconvoluted into a triplet at g_{iso1} 1.9792 ($a_H = 1.0 \times 10^{-4}$ cm^{-1}), a quintet at g_{iso2} 1.9794 ($a_H = 0.9 \times 10^{-4}$ cm^{-1}) and a septuplet at g_{iso3} 1.9793 ($a_H = 1.0 \times 10^{-4}$ cm^{-1}), in 6:3:1 ratio. Other minor species were also present, but they were not included in the simulations to avoid over-parameterization. Based on the shf coupling, the three components could correspond to [Cr(O)(*cis*-O^1,O^2Glc3Me)$_2$] (**II**), [Cr(O)(*cis*-O^1,O^2-Glc3Me)(O^5,O^6-Glc3Me-furanose)] (**III**) and [Cr(O)(O^5,O^6-Glc3Me-furanose)$_2$] (**IV**) (Fig. 4). At longer times, the proportion of the species at g_{iso1} decreased and the spectra were dominated by species at g_{iso2} and g_{iso3}. These five-coordinate Cr^{V} bis-chelates were still observed 15 h after mixing. Thus, initially, Cr^{V} bis-chelate is formed with Cr^{V} bound to the 1,2-*cis*-diolato moiety of the pyranose form of Glc3Me (kinetic control); but, with time, it transforms into bis-chelates with Cr^{V} bound to the 5,6-*vic*-diolato moiety of the furanose form of the ligand.

3.5. Rate studies

The kinetics of the reaction of Glc3Me with Cr^{VI} was examined by monitoring the [Cr^{VI}] consumption under conditions of excess of Glc3Me over Cr^{VI}, in the 0.15–1.02 mol/L $HClO_4$ range. UV–Vis spectra of the reaction mixtures showed an absorbance band at 350 nm and a shoulder at 420–500 nm, characteristic of Cr^{VI} in acidic medium. At 350 nm, the absorbance versus time curves exhibited a monotonic decrease and the rate constants were calculated from the absorbance changes at this wavelength. As stated before, Cr^{V} species are formed in the chromic oxidation of Glc3Me, and it is known that these species absorb at 350 nm and may superimpose Cr^{VI} absorbance [35]. However, if Cr^{V} reacts faster than Cr^{VI} and exists in solution in a sufficiently small concentration, changes in absorbance at 350 nm essentially reflect changes in Cr^{VI} concentration. The relative values of the Cr^{VI} versus Cr^{V} reduction rate constants obtained from the Cr^{V} EPR signal intensity variation during the reaction course demonstrated this is the case for the reaction studied here (discussed below).

The kinetic profiles at 350 nm could be adequately described by a single exponential decay from which Cr^{VI} pseudo-first order rate constants (k_{exp}) were calculated. Table 1 summarizes values of k_{exp} for various concentrations of Glc3Me and $HClO_4$. Plots of k_{exp} versus [Glc3Me] at constant [H^+] gave good straight lines (Fig. 6) from which values of k_h were determined (Table 1, right). Values of k_h showed quadratic dependence on [H^+] (Fig. 6, inset), and the rate constant k_6, calculated by non-linear least-square fit of {k_h, [H^+]} data pairs, was found to be $(6.35 \pm 0.02) \times 10^{-4}$ mol^{-3} L^3 s^{-1}. Consequently, the complete rate law for the Cr^{VI} consumption can be expressed as in Eq. (1):

$$-d[Cr^{VI}]/dt = k_6[H^+]^2[Glc3Me][Cr^{VI}]. \quad (1)$$

Table 1
Experimental pseudo-first-order rate constants (k_{exp})[a] for different concentrations of Glc3Me and $HClO_4$.

[$HClO_4$] (mol/L)	10^5 k_{exp} (s^{-1}) for [Glc3Me] (mol/L)					
	0.04	0.08	0.12	0.16	0.20	10^4 k_h (mol^{-1} L s^{-1})
0.15		1.94(1)	2.58(3)	2.94(3)	4.09(8)	2.0(1)
0.31	3.12(1)	6.19(3)	8.23(9)	10.4(3)	14.4(1)	7.0(2)
0.46	6.51(4)	12.4(1)	17.7(1)	22.0(4)	28.4(1)	14.3(3)
0.61	10.9(2)	20.1(1)	31.0(2)	40.2(1)	49.9(9)	25.2(2)
0.77	15.8(4)	29.9(3)	44.4(6)	59.2(1)	72.4(2)	36.7(3)
0.92	22.8(3)	44.5(1)	63.6(9)	84.0(7)	106(1)	53.1(5)
1.02	27.0(4)	53.2(1)	78.5(4)	104(1)	135(1)	66.4(6)

[a] Mean values from multiple determinations. $[Cr^{VI}]_0 = 6 \times 10^{-4}$ mol/L, T = 33 °C; I = 1.02 M, λ_{350}.

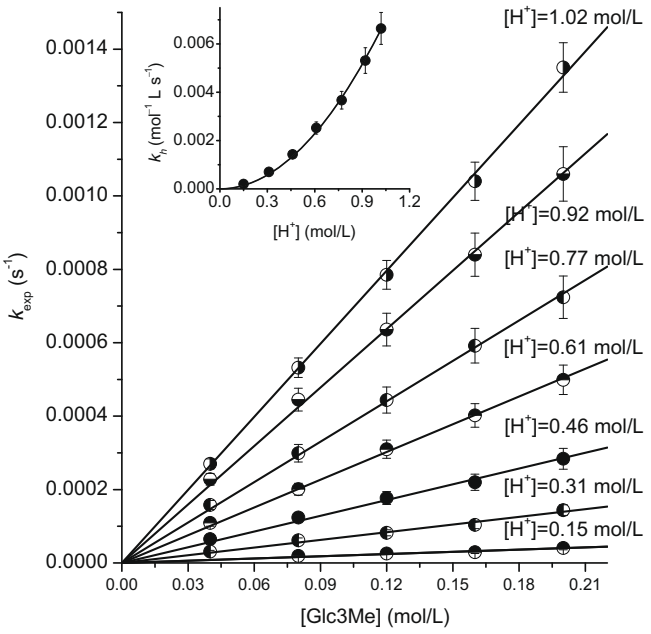

Fig. 6. Effect of [Glc3Me] on k_{exp} at 33 °C, I = 1.02 mol/L, λ = 350 nm and different [H$^+$]. Inset: dependence of k_h on [H$^+$].

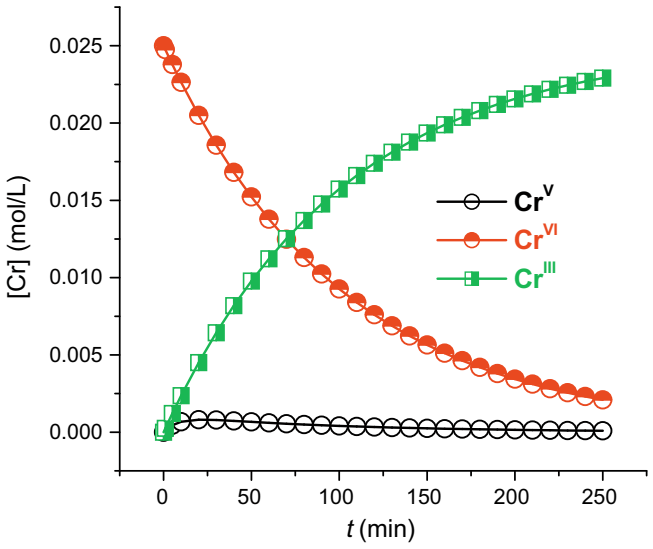

Fig. 7. Simulated kinetic profiles for Cr species. [Cr] calculated using k_a = 0.00496 min^{-1} and k_b = 0.1224 min^{-1} obtained from EPR data in 0.3 mol/L $HClO_4$. [Cr]$_T$ = 0.025 mol/L.

The kinetic results were independently confirmed by following the redox reaction by EPR spectroscopy. Fig. 3 shows a typical curve for the growth and decay of the Cr^V EPR signal peak-to-peak height as a function of time. The kinetic profiles could be adequately fitted with the rate expression derived from a two-step reaction sequence involving two consecutive first-order reactions (Scheme 2 and Eq. (2)) [11,36]:

$$EPR_{area} = Ak_a\{\exp(-2k_at) - \exp(-k_bt)\}/(k_b - 2k_a), \quad (2)$$

where A depends on the spectrometer settings, and k_a and k_b refer to the rate of disappearance of Cr^{VI} and Cr^V, respectively, and were evaluated from a non-linear least-squares fit of Eq. (2). In the 0.3 to 0.5 mol/L $HClO_4$ range, the calculated values of k_a were more than ten-times lower than k_b. For conditions in Fig. 3, k_a = 0.00496 min^{-1} and k_b = 0.1224 min^{-1}. The fact that $k_b > k_a$ implies that the slow redox step involves the reduction of Cr^{VI}. The simulation of the kinetic profiles employing k_a and k_b values obtained from EPR data in 0.3 mol/L $HClO_4$ (Fig. 7), shows that the maximal [Cr^V] represents 3% of the total Cr in solution. These results confirm that [Cr^V] is low throughout the reaction and should not interfere absorbance at 350 nm, which essentially reflects changes in [Cr^{VI}]. Rate constants calculated by this technique were consistent with those obtained from the spectrophotometric measurements at 350 nm, under the same experimental conditions. For 1.225 mol/L Glc3Me and 0.3 mol/L $HClO_4$, the value determined spectrophotometrically for k_{exp} was 1.90×10^{-4} s^{-1}, that compares well with $2k_a = 1.65 \times 10^{-4}$ s^{-1} obtained from EPR measurements.

Sequential absorption spectra of the reaction mixture showed the appearance and growth of two d–d bands at λ_{max} = 409 and 572 nm (Fig. 8). Kinetics traces at 570 nm showed that at this wavelength, the absorbance grew to intensities higher than expected for the free Cr^{3+} and then slowly decayed to the value corresponding to $[Cr(H_2O)_6]^{3+}$ (409 nm, ε = 17.7 mol^{-1} L cm^{-1} and 572 nm, ε = 15.2 mol^{-1} L cm^{-1}) [37], as shown in the inset of Fig. 8. This behavior suggests the formation of an intermediate Cr^{III}–Glc3Me complex, which then hydrolyzes to the final product [30,38]. EPR spectra taken at the end of the reaction confirm that Cr^{3+} is the final Cr species in the reaction of Cr^{VI} with excess Glc3Me in acid medium.

In order to determine the rate of Cr^{III} formation relative to that of the Cr^{VI} consumption, the formation of Cr^{III} was followed at 570 nm, in the presence of excess of Glc3Me in the 0.40–1.02 mol/L $HClO_4$ concentration range. Under these conditions, the first order dependence of the rate upon [Cr^{VI}] was verified. For [Glc3Me]$_0$ = 0.4 mol/L, values of k_{exp} calculated at this wavelength

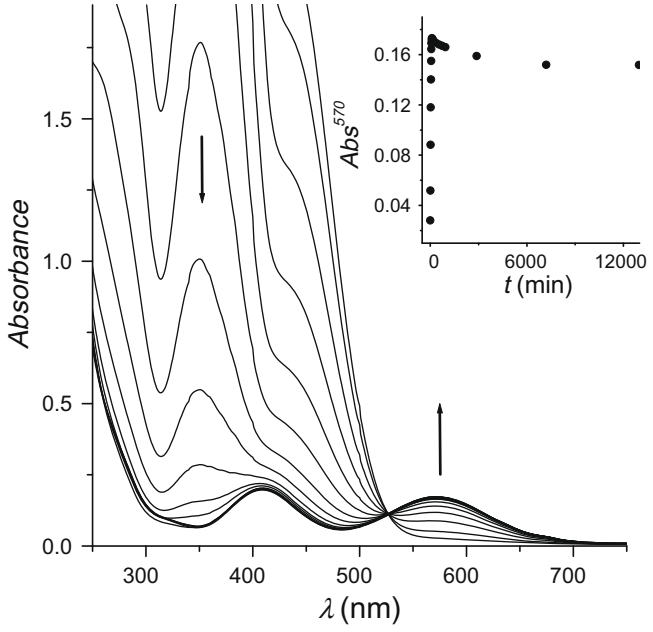

Fig. 8. Time evolution of the UV–Vis spectra of a mixture of 0.4 mol/L Glc3Me and 0.01 mol/L Cr^{VI} over a period of 16 h. [$HClO_4$] = 1.02 mol/L, T = 33 °C. Inset: growth and slow decay of Abs^{570} over a period of 9 days.

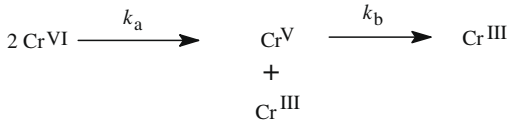

Scheme 2.

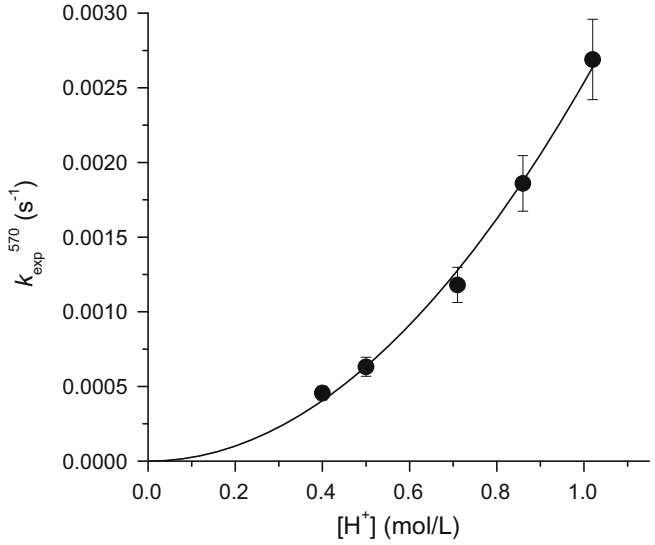

Fig. 9. Effect of acidity on k_{exp} calculated from absorbance data at 570 nm. $[Cr^{VI}] = 8 \times 10^{-3}$ mol/L, [Glc3Me] = 0.4 mol/L, I = 1.02 mol/L, T = 33 °C.

were plotted against $[H^+]$ (Fig. 9). The rate constant calculated by non-linear least-square fit of $\{k_{exp}, [H^+]\}$ data pairs was found to be 25.4×10^{-4} mol^{-2} L^2 s^{-1}, which is the same as that calculated from data at 350 nm. This indicates that the rate of formation of Cr^{III} equals the rate of consumption of Cr^{VI} and that the slow redox path effectively implies the reduction of Cr^{VI}, which should react slower than Cr^V does. This is also consistent with the observation of an isosbestic point at 527 nm (Fig. 8) and implies a low Cr^V concentration throughout the reaction in the $[H^+]$ range used in the kinetics studies.

3.6. Mechanism of the Glc3Me + Cr^{VI} reaction

In the range of substrate and acid concentration used in the kinetics measurements, the oxidation of Glc3Me by Cr^{VI} is a complex reaction that yields Cr^{III}, HCO_2H and Ara2Me as final redox products. The fact that CrO_2^{2+} is detected in the reaction of Glc3Me with Cr^{VI} together with the observation of Cr^V species and the successful trap of organic radicals using acrylamide indicates that the reaction occurs through both one- and two-electron pathways involving Cr^{IV} and Cr^V intermediate species. However, under conditions used in the kinetic measurements, Cr^{IV} and Cr^V react with Glc3Me faster than Cr^{VI} and do not accumulate in the reaction mixture. Therefore, Cr^{IV} and Cr^V, although formed in the Cr^{VI} + Glc3Me, should be involved in fast steps of the reaction pathway. Thus, the absorbance-time profiles reflect the $[Cr^{VI}]$ monotonic decay (at 350 nm) or the $[Cr^{III}]$ monotonic growth (at 570 nm) without interference of $[Cr^{IV}]$ or $[Cr^V]$. In Scheme 3, we propose a mechanism that combines $Cr^{VI} \rightarrow Cr^{IV} \rightarrow Cr^{II}$ and $Cr^{VI} \rightarrow Cr^{IV} \rightarrow Cr^{III}$ pathways, and takes into account: (a) kinetic results, (b) the polymerization of acrylamide added to the reaction mixture, (c) detection of intermediate of Cr^{VI} esters and oxochromate(V) species, (d) observation of CrO_2^{2+} and (e) the reaction products.

The first step of the mechanism proposed in Scheme 3 involves the formation of a Glc3Me–Cr^{VI} mono-chelate (Eq. 3), in agreement with the observation of the absorption band at 373 nm characteristic of chromate oxo-ester, immediately after mixing Glc3Me and Cr^{VI} under conditions where the redox reaction is extremely slow. Therefore, such a chromate ester should be formed rapidly prior to the redox steps. The formation of the chromate ester is followed by the slow redox step where the C–C bond cleavage is proposed to occur through an acid catalyzed two-electron redox process to

$$\text{Glc3Me} + Cr^{VI} \underset{}{\overset{\text{fast}}{\rightleftharpoons}} \text{Glc3Me-}Cr^{VI} \quad (3)$$

$$\text{Glc3Me-}Cr^{VI} \xrightarrow{k_6,\ 2\,H^+} Cr^{IV} + HCO_2H + \text{Ara2Me} \quad (4)$$

$$Cr^{IV} + \text{Glc3Me} \xrightarrow{\text{fast}} Cr^{III} + HCO_2H + \text{Glc3Me}^{\bullet} \quad (5)$$

$$Cr^{IV} + \text{Glc3Me} \xrightarrow{\text{fast}} Cr^{II} + HCO_2H + \text{Ara2Me} \quad (6)$$

$$Cr^{II} + Cr^{VI} \xrightarrow{\text{fast}} Cr^{V} + Cr^{III} \quad (7)$$

$$Cr^{VI} + \text{Glc3Me}^{\bullet} \xrightarrow{\text{fast}} Cr^{V} + \text{Ara2Me} + HCO_2H \quad (8)$$

$$\text{Glc3Me} + Cr^{V} \xrightarrow{\text{fast } (k_b)} Cr^{III} + HCO_2H + \text{Ara2Me} \quad (9)$$

$$Cr^{II} + O_2 \xrightarrow{\text{fast}} CrO_2^{2+} \longrightarrow Cr^{III} \quad (10)$$

$$O_2 + \text{Glc3Me}^{\bullet} \xrightarrow{\text{fast}} \text{Glc3Me}_{ox} \quad (11)$$

Scheme 3.

yield Cr^{IV}, HCO_2H and Ara2Me (Eq. 4). The initial two-electron reduction of Cr^{VI} by Glc3Me is in agreement with previous reports on a number of oxygenated compounds that were selectively oxidized by Cr^{VI} to the lower homolog [30,35]. In the mechanism, we have included two competitive one- and two-electron reductions of Cr^{IV} by Glc3Me. Thus, Cr^{IV} is proposed to react with excess Glc3Me to yield Cr^{III}, HCO_2H and Glc3Me$^{\bullet}$, or Cr^{II}, HCO_2H and Ara2Me, through two alternate fast steps (Eqs. 5 and 6). The first is supported by the observed polymerization of acrylamide when it is added to the Cr^{VI}/Glc3Me reaction mixture, while the second, by the observation of CrO_2^{2+} (the product of the reaction of Cr^{II} with O_2). Cr^V can form by fast reaction of Cr^{II} with Cr^{VI} (Eq. 7) and, alternatively, by rapid reaction of the Glc3Me$^{\bullet}$ with Cr^{VI} (Eq. 8). Cr^V can further oxidize Glc3Me to yield Cr^{III}, HCO_2H and Ara2Me as final redox products (Eq. 9). In the mechanism, one half of the Cr^{VI} reaches Cr^{III} through the Cr^V intermediate, in accordance with Scheme 2 used to fit the time evolution of the Cr^V EPR signal.

In O_2-saturated solutions (1.26 mmol/L) and $[Cr^{VI}]_0 < 0.1$ mmol/L, reactions 7 and 8 can be neglected because Glc3Me$^{\bullet}$ and Cr^{II} intermediates formed in reactions 5 and 6 should be rapidly trapped by O_2 (reactions 10 and 11) [39]. The proposed mechanism is in accordance with the observation that O_2 has not kinetic effect on this reaction, because when $[Cr^{VI}]_0 \geqslant 0.5$ mmol/L (as employed in the kinetic measurements), both Cr^{II} and Glc3Me$^{\bullet}$ react with Cr^{VI} faster than they do with O_2, and reactions 10 and 11 can be neglected [27,40,41].

4. Conclusion

The reaction of Glc3Me with Cr^{VI} strongly depends on pH. In acid medium, redox reaction occurs and reactive Cr^V, Cr^{II} and Cr^{IV} intermediate species are generated in the redox process, together with free radicals, HCO_2H and Ara2Me. At pH > 3, Glc3Me oxidation by Cr^{VI} or Cr^V is very slow and long-lived oxo-Cr^{VI} or oxo-Cr^V–Glc3Me species form. EPR spectroscopy shows that at pH 5.5–7.5 Glc3Me is able to trap Cr^V through the 1,2-diolato moiety to yield

a Cr^V bis-chelate that then slowly converts into species with Cr^V bound to the 5,6-diolato moiety of its furanose form. The selective C1–C2 bond cleavage of Glc3Me upon reaction with high valent chromium in acid medium, distinguishes the 3-OMe derivative from glucose that, under the same experimental conditions, is oxidized to the gluconic acid at comparable rate [10].

Acknowledgments

We thank the National Research Council of Argentina (CONICET), the National University of Rosario (UNR), the National Agency for Sciences Promotion (FONCyT) and the ALFA Program (CROCON Network, Project ALR/B7-30.11/94-7.0064.9) for financial support. MIF thanks V. Andreu for helping with the kinetic measurements.

References

[1] J. Barnhart, J. Soil Contam. 6 (1997) 561 (special issue).
[2] S.A. Katz, H. Salem, in: The Biological and Environmental Chemistry of Chromium, VCH Publishers, Inc., New York, 1994.
[3] C.B. Klein, in: L.W. Chang (Ed.), Toxicology of Metals, CRC-Lewis Publishers, New York, 1996, p. 205.
[4] R. Codd, C.T. Dillon, A. Levina, P.A. Lay, Coord. Chem. Rev. 216–217 (2001) 537.
[5] R. Codd, J.A. Irwin, P. Lay, Curr. Opin. Chem. Biol. 7 (2003) 213.
[6] A.K. Das, Coord. Chem. Rev. 248 (2004) 81.
[7] M. Ciéslak-Golonka, M. Daszkiewicz, Coord. Chem. Rev. 249 (2005) 2391.
[8] B. Gyurcsik, L. Nagy, Coord. Chem. Rev. 203 (2000) 81.
[9] S. Signorella, J.C. González, L.F. Sala, J. Argentine Chem. Soc. 90 (2002) 1.
[10] S. Signorella, V. Daier, S. García, R. Cargnello, J.C. González, M. Rizzotto, L.F. Sala, Carbohydr. Res. 316 (1999) 14.
[11] V. Daier, S. Signorella, M. Rizzotto, M. Frascaroli, C. Palopoli, C. Brondino, J.M. Salas-Peregrin, Can. J. Chem. 77 (1999) 57.
[12] M. Rizzotto, S. Signorella, M.I. Frascaroli, V. Daier, L.F. Sala, J. Carbohyd. Chem. 14 (1995) 45.
[13] S. Signorella, M. Rizzotto, V. Daier, M.I. Frascaroli, C. Palopoli, D. Martino, A. Bousseckson, L.F. Sala, J. Chem. Soc., Dalton Trans. (1996) 1607.
[14] M. Rizzotto, M. Frascaroli, S. Signorella, L. Sala, Polyhedron 15 (1996) 1517.
[15] M. Krumpolc, J. Rocek, Inorg. Synth. 20 (1980) 63.
[16] M.C. Ghosh, E.S. Gould, Inorg. Chem. 30 (1991) 491.
[17] International Agency for Research on Cancer (IARC), IARC Monogr. Eval. Carcinog. Risk Chem. Hum. (Suppl. 7) (1987) 165.
[18] R.Feldam, in: Occupational and Environmental Neurotoxicology, Lippincott-Raven Publishers, Philadelphia, 1999, p. 337.
[19] L.F. Sala, A. Fernández Cirelli, R.M. Lederkremer, Anales Asoc. Química Arg. 66 (1978) 57.
[20] H.S. Isbell, J. Res. Nat. Bur. Stand. (US) 14 (1935) 305.
[21] A.G. Fadnis, S.K. Kulshrestha, Rev. Roumaine Chim. 28 (1983) 99.
[22] S.L. Scott, A. Bakac, J.H. Espenson, J. Am. Chem. Soc. 113 (1991) 7787.
[23] WINSIM EPR Calculations for MS-Windows NT, Version 0.96, National Institute of Environmental Health Sciences, 1995.
[24] M. Mitewa, P. Bontchev, Coord. Chem. Rev. 61 (1985) 241.
[25] J.C. González, S. García, N. Mamana, L.F. Sala, S. Signorella, Inorg. Chem. Commun. 9 (2006) 437.
[26] S.L. Scott, A. Bakac, J.H. Espenson, J. Am. Chem. Soc. 114 (1992) 4205.
[27] S. Signorella, M.I. Frascaroli, S. García, M. Santoro, J.C. González, C. Palopoli, N. Casado, L.F. Sala, J. Chem. Soc., Dalton Trans. (2000) 1617.
[28] A. Al-Ajlouni, A. Bakac, J. Espenson, Inorg. Chem. 33 (1994) 1011.
[29] S. Signorella, M. Santoro, C. Palopoli, C. Brondino, J.M. Salas Peregrin, M. Quiroz, L. Sala, Polyhedron 17 (1998) 2739.
[30] G. Barr-David, M. Charara, R. Codd, R.P. Farrell, J.A. Irwin, P.A. Lay, R. Bramley, S. Brumby, J.Y. Ji, G.R. Hanson, J. Chem. Soc., Faraday Trans. 91 (1995) 1207.
[31] A. Levina, P.A. Lay, Coord. Chem. Rev. 249 (2005) 281.
[32] M. Rizzotto, A. Levina, M. Santoro, S. García, M.I. Frascaroli, S. Signorella, L.F. Sala, P. Lay, J. Chem. Soc., Dalton Trans. (2002) 3206.
[33] S. Signorella, V. Daier, M. Santoro, S. García, C. Palopoli, L. Korecz, A. Rockenbauer, L.F. Sala, Eur. J. Inorg. Chem. (2001) 1829.
[34] S. Signorella, S. García, M. Rizzotto, A. Levina, P. Lay, L.F. Sala, Poyhedron 24 (2005) 1079.
[35] G. Haight, G. Jwisich, M. Kelso, P. Merril, Inorg. Chem. 24 (1985) 2740.
[36] V. Roldán, M. Santoro, J.C. González, J.M. Salas Peregrin, S. Signorella, L.F. Sala, J. Inorg. Biochem. 98 (2004) 347.
[37] A.B.P. Lever, in: Inorganic Electronic Spectroscopy, 2nd Ed., Elsevier, Amsterdam, 1984, p. 419.
[38] S. Signorella, M. Santoro, A. Frutos, G. Escandar, J.M. Salas-Peregrin, V. Moreno, M. González Sierra, L.F. Sala, J. Inorg. Biochem. 73 (1999) 93.
[39] A. Bakac, S.L. Scott, J.H. Espenson, K.R. Rodgers, J. Am. Chem. Soc. 117 (1995) 6483.
[40] O. Pestovsky, A. Bakac, J.H. Espenson, J. Am. Chem. Soc. 120 (1998) 13422.
[41] P.A. Lay, A. Levina, J. Am. Chem. Soc. 120 (1998) 6704.